Low-coherence fiber-optic sensor ring network based on a Mach–Zehnder interrogator

Libo Yuan

Department of Physics, Harbin Engineering University, Harbin 150001, China

Limin Zhou

Department of Mechanical Engineering, The Hong Kong Polytechnic University, Hong Kong, China

Wei Jin

Department of Electrical Engineering, The Hong Kong Polytechnic University, Hong Kong, China

Jun Yang

Photonics Research Center, Harbin Engineering University, Harbin 150001, China

A quasi-distributed fiber sensor system for smart-structure applications is proposed. The system is based on a fiber loop topology and interrogated by use of white-light interferometry. The results of preliminary experiments and a power budget analysis are presented.   © 2002 Optical Society of America

OCIS codes: 060.2370, 060.4230, 060.4250, 120.3180.

In smart-structure applications, in which fiber sensors are embedded within structural materials,[1-3] multiple lead-in–out fibers are preferred for redundancy and improved reliability. The use of only one lead-out fiber is not optimal because the breakage of fiber at one location, for example, because of local structural damage, would cause the failure of the whole sensing system. Multiplexing and networking techniques that are suitable for such applications attracted considerable research recently.[4-9] In this Letter we report the results of our recent investigation on the networking of white-light interferometric sensors based on a fiber-optic Sagnac loop, which has been designed to satisfy the needs of redundancy for large-scale smart structures.

Figure 1 shows the proposed sensor system, where N sensing segments (N sensors) are connected in series with partial reflectors between the adjacent sensors. Each end of the sensing fiber is connected to an arm of a coupler to allow for interrogation of each sensor from opposite directions through the use of both ends at the same time. Sensor interrogation is achieved through the use of a scanning Mach–Zehnder interferometer (MZI) powered by a LED. The gauge lengths of the sensors ($l_1, l_2, \cdots, l_N$) are chosen to be slightly different from one another but approximately the same as the optical path-length difference (OPD) of the MZI. The OPD of the MZI can be tuned through the use of a scanning prism graded-index (GRIN) lens system. When the prism is tuned to a position where the OPD of the MZI is matched to the gauge length of a particular sensor, a white-light interferometric pattern is generated. Take sensor j as an example: The pairs of matching paths are shown in Fig. 2. The pair shown at the top corresponds to interrogation of the sensor via the clock-wise direction, and the pair shown at the bottom is for interrogation via the counterclockwise direction. OPD matching is achieved at the same time for both pairs of paths when

$$n\Delta L_0 + 2X_j = nl_j, \tag{1}$$

where $n\Delta L_0$ is the OPD of the MZI without including the gap between the prism and the GRIN lenses and can be kept constant if the MZI is kept within a heat-isolated box. We have selected ΔL_0 to be nearly equal to l_j so that the prism does not need to be moved much further to match the optical path. $X = X_j$ is the gap distance between the prism and the GRIN lenses, as shown in Fig. 1. Applied strain or temperature will cause a change in nl_j that requires a change in the gap distance, X_j, so that the condition given in Eq. (1) is satisfied. The variation in the gap distance (ΔX_j) is related to gauge length change by $\Delta X_j = \Delta(nl_j)/2$.

The experiment was conducted with four-sensor network ($N = 4$ in Fig. 1). The LED used had a center wavelength of 1310 nm and an output power of 50 μW. The insertion losses of the GRIN lens–prism system
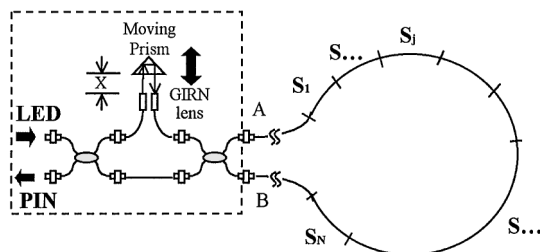

Fig. 1. Fiber-optic white-light interferometric strain sensors connected in a loop configuration. PIN, p-i-n diode.
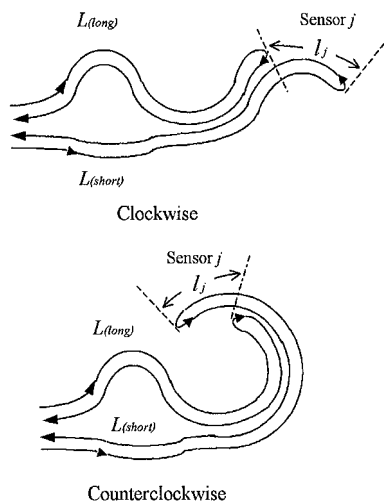
Fig. 2. Optical paths and reflective signals for sensor j. $L_{(\text{long})}$ represents the arm of the MZI with the prism and the GRIN lenses.

were within range 4–8 dB, with a scanning range of ~15 cm (corresponding to a 30-cm OPD change). The gauge length of each of the four sensors was ~100 mm, and all fiber sensors were butt connected to each other. The photodetector output when the value of X was varied from 2.5 to 22.5 mm is shown in Fig. 3. The four major peaks correspond to the OPDs of the MZI being matched to the four sensors. From Fig. 3, it is obvious that the gauge length of the sensors satisfies $l_3 < l_2 < l_1 < l_4$. The experiment was repeated with one end of the fiber loop disconnected from the loop coupler. Although the amplitudes of the peaks varied, the positions of the peaks were found not to change, indicating the potential of the system for structural monitoring applications even if one end of the fiber is broken.

To estimate the number of sensors that can be multiplexed with the proposed topology, we assume that the light power launched into the fiber is P_0 and the minimum power that can be detected by the photodiode is $P_{\min}$. The signal intensity from sensor j that is due to coherent mixing between the reflected signals from the two partial reflectors that define the sensor can be expressed as

$$P_D(j) = \frac{1}{8} P_0 \eta(X_j) \Bigg\{ (R_j R_{j+1} T_j \beta_j T_j' \beta_j')^{1/2}$$

$$\times \left(\prod_{i=1}^{j-1} T_i \beta_i \right) \left(\prod_{i=1}^{j-1} T_i' \beta_i' \right)$$

$$+ (R_j' R_{j+1}' T_{j+1} \beta_{j+1} T_{j+1}' \beta_{j+1}')^{1/2}$$

$$\times \left(\prod_{i=j+2}^{N+1} T_i \beta_i \right) \left(\prod_{i=j+2}^{N+1} T_i' \beta_i' \right) \Bigg\}, \qquad (2)$$

where the two couplers are assumed to be 3-dB couplers and the insertion losses are neglected. β_j represents the excess loss associated with sensor j

because of, for example, connection loss, absorption loss, and other strays between the sensing segments. T_j and R_j are, respectively, the transmission and reflection coefficients of the jth partial reflector. T_j is in general smaller than $1 - R_j$ because of loss factor β_j. $\eta(X_j)$ is the loss associated with the prism–GRIN lens system and is a function of X_j. β_j', T_j', and R_j' represent, respectively, the loss, transmission, and reflection from the counterclockwise direction.

Simulations were conducted for typical parameters: $\beta_j = \beta_j' = 0.9$ ($j = 1, 2, \ldots, N + 1$), $R_j = R_j' = 1\%$, and $T_j = T_j' = 0.89$. The average attenuation of the moving prism–GRIN lens part is taken as 6 dB, i.e., $\eta(X_j) = 1/4$. The power coupled into the input fiber is $P_0 = 50$ μW. The normalized output signals of the four fiber-optic sensors are shown in Fig. 4 for evaluation of the differences between the connected and the disconnected cases of the sensor ring network. The optical signal intensity of each of the sensors in the array for different array sizes is shown in Fig. 5. Assuming that $P_{\min} = 10$ nW, the condition $P_D(j) \geq P_{\min}$ (for all j) allows four sensors to be multiplexed for light
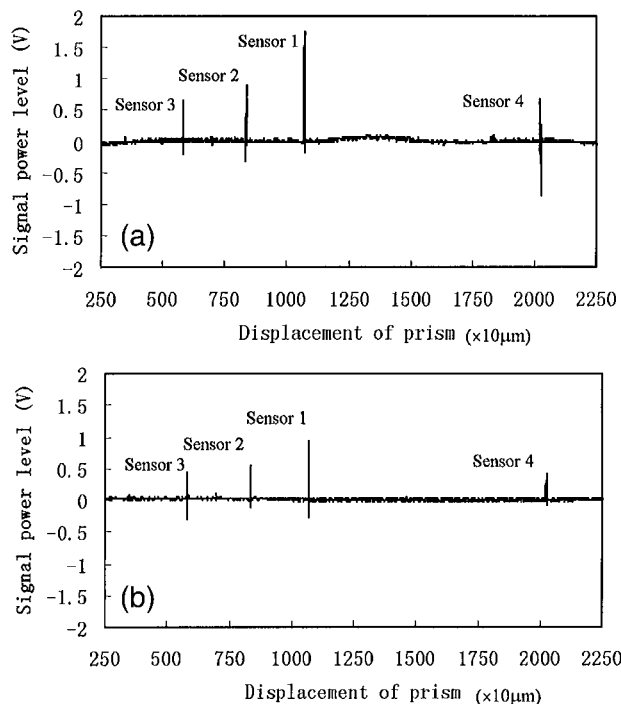

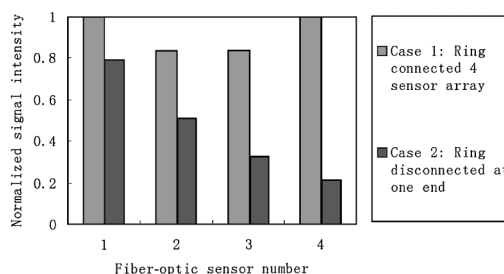Fig. 3. System output of the four-sensor array.

Fig. 4. Simulation results of the fiber-optic sensor versus the normalized signal intensities with the ring array connected and with the ring disconnected at end B of the loop (see Fig. 1).
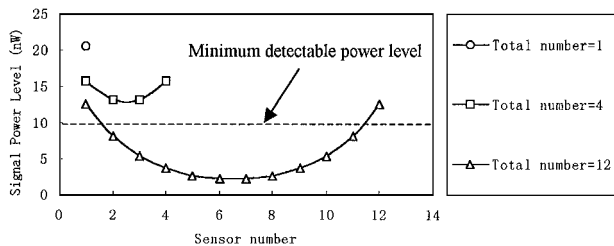
Fig. 5.   Signal power of each of the sensors for different array-size (total number of sensors) simulation results with light source power $P_0 = 50 \ \mu$W.
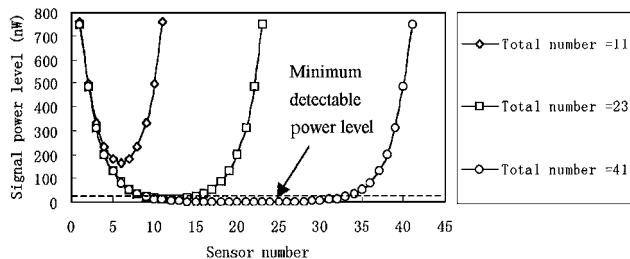

Fig. 6.   Signal power of each of the sensors for different array-size (total number of sensors) simulation results with light source power $P_0 = 3$ mW.

source power $P_0 = 50 \ \mu$W. The number of sensors could be increased to 23 if a 3-mW light source were used. For that case, the simulation results are given in Fig. 6.

The maximum number of sensors may be limited by other factors, e.g., the available moving range of the scanning prism system. In addition, the receiver noise floor, and hence the detection sensitivity, would be a function of detector bandwidth, which depends on the required response time of the system and the scanning speed of the moving prism. For a specific sys-tem, a detailed analysis considering all these aspects is needed for full assessment of the multiplexing capacity of the topology.

In summary, a fiber-optic sensor ring network suitable for embedded applications has been demonstrated. The sensor system is based on multiplexed white-light interferometers connected in a loop topology. The system worked well even when one end of the loop was disconnected, indicating the potential of the system for applications in which redundancy is needed. Budget analysis showed that an array of more than 20 sensors could be realized with a 3-mW broadband source.

References

1. A. D. Kersey and W. W. Morey, Electron. Lett. **29,** 112 (1993).
2. G. Duck and M. M. Ohn, Opt. Lett. **25,** 90 (2000).
3. E. Sensfelder, J. Burck, and H. J. Ache, Appl. Spectrosc. **52,** 1283 (1998).
4. V. Lecoeuche, D. J. Webb, C. N. Pannell, and D. A. Jackson, Opt. Commun. **168,** 95 (1999).
5. W. V. Sorin and D. M. Baney, IEEE Photon. Technol. Lett. **7,** 917 (1995).
6. L. B. Yuan and F. Ansari, Sensors Actuators A **63,** 177 (1997).
7. L. B. Yuan, L. Zhou, and W. Jin, Opt. Lett. **25,** 1074 (2000).
8. J. M. Senior, S. E. Moss, and S. D. Cusworth, Opt. Laser Technol. **28,** 1 (1996).
9. W. Ecke, I. Latka, R. Willsch, A. Reutlinger, and R. Graue, Meas. Sci. Technol. **12,** 974 (2001).